J Solid State Electrochem (2010) 14:989–995
DOI 10.1007/s10008-009-0887-1

ORIGINAL PAPER

Silver electrodeposition from water–acetonitrile mixed solvents. Part III—an in situ investigation by optical second harmonic generation spectroscopy

Elisabetta Tondo · Claudio Mele · Benedetto Bozzini

Received: 5 May 2009 / Revised: 15 June 2009 / Accepted: 15 June 2009 / Published online: 23 July 2009

Abstract In this work, we report an investigation based on silver electrodeposition from water–acetonitrile mixed solvents onto a polycrystalline Au electrode, based on in situ optical second harmonic generation (SHG) spectroscopy. This paper is the last one of a series attacking the same topic by cyclic voltammetry and potentiostatic current transients (Mele et al., J Solid State Electrochem in press, 1) and in situ surface-enhanced Raman scattering (Mele et al., J Solid State Electrochem in press, 2). SHG intensity transients following the application of potentiostatic cathodic steps have been measured in order to obtain detailed information on the formation of Ag clusters and nuclei during the electrodeposition process. Our SHG data have been rationalised in terms of a simple optical model accounting for SHG enhancement brought about by Ag cluster formation.

Introduction

Many researches have been carried out showing that second harmonic generation (SHG) is an ideal spectroscopic technique for examining electrochemical interfaces in aqueous media, in particular in terms of adsorption of molecules, ions, metal atoms and reaction intermediates at metal electrodes (i.e. [1] and references therein contained). This technique, of course, is also suitable to investigate the metal/electrolyte interface in non-aqueous systems. This topic has recently gained growing interest, because the use of non-aqueous or mixed solvents offers an alternative route for several electrochemical processes, allowing limited influence of water-related electrochemical reactions, as well as the possibility of solubilising many organics [2, 3]. The study of the interfacial electrochemistry of Ag/H_2O/acetonitrile (CH_3CN) systems has received some attention in the literature [4–6]. However, limited research effort was gone so far in the electrodeposition from non-aqueous phases [7–9]. In [10], a selection of non-aqueous solvent-based plating systems has been reviewed. Some surface-enhanced Raman scattering (SERS) studies of silver [5, 11] and platinum [4] in acetonitrile solutions have been also performed, but to the best of the authors' knowledge, no SHG electrochemical work has been reported concerning electrodeposition from mixed solvents.

This paper is part of a series addressing the topic of Ag electrodeposition from water–acetonitrile mixed solvents. In the previous papers of this series [11, 12], we investigated the nucleation of silver by electrochemical methods (cyclic voltammetry and potentiostatic current transients), the nucleation and growth morphology by scanning electron microscopy and the metal/electrolyte interface composition by SERS spectroscopy. In the present paper, we use in situ SHG in order to monitor the formation of Ag clusters and nuclei, giving rise to changes in SHG signal intensity (I_{SHG}).

Experimental

The electrodeposition baths we employed were (a) $AgNO_3$ 10 mM, $NaClO_4$ 0.1 M and 100% H_2O; (b) $AgNO_3$ 10 mM, $NaClO_4$ 0.1 M, 50% H_2O and 50% CH_3CN and (c) $AgNO_3$ 10 mM, $NaClO_4$ 0.1 M and 100% CH_3CN. The solutions were prepared from analytic grade chemicals and ultra-pure water with a resistivity of 18.2 MΩ cm. In the electrochemical literature, ClO_4^- is often regarded as an

E. Tondo · C. Mele · B. Bozzini (✉)
Dipartimento di Ingegneria dell'Innovazione, Salento University,
via Monteroni,
Lecce 73100, Italy
e-mail: benedetto.bozzini@unile.it

inert ion: Nevertheless, if the presence of Cl^- is expected to impact the relevant experiments, careful attention should be given to the possibility of reduction of perchlorate to chloride. [13] reports work on a Ni electrode in contact with 0.1 M $HClO_4$, showing that at room temperature, the formation of Cl^- is vanishing in a wide potential range, whilst at −0.9 V_{SCE} at T>55°C, it becomes sizable. [14] has found that Cl^- can form at room temperature in solutions with $HClO_4$ concentrations in excess of 1 M in a wide range of electrochemical conditions, the mildest ones—in the presence of a catalytic cathode—being potential pulsing between 0 and −0.2 V_{RHE}. Catalytic effects have been discussed for many metals, but Ag does not seem to have been studied. Furthermore, in the case of Cl^--adsorbing cathodes, such as Pt, adsorption has been proved to inhibit further ClO_4^- reduction. Moreover, an acidic environment seems critical for the reduction of ClO_4^- to Cl^- [15]. Since—in the present investigation—we used a neutral system at room temperature with comparatively low concentrations of ClO_4^-, polarisations≥−0.6 $V_{Ag/AgCl}$ and, moreover, our aqueous baths are $AgNO_3$ solutions (accumulation of Cl^- would be impeded by the precipitation of AgCl), we have sufficient reasons to believe that the formation of Cl^- is negligible.

The SHG spectrometer, optics and control electronics were constructed in our laboratory; for details, see [16]. An yttrium lithium fluoride laser (wavelength 1,064 nm) was used, the optical second-harmonic was collected by a photomultiplier tube and its reading was ratioed to a reference channel based on a photodiode. SHG experiments were performed at 50° incidence angle with *p*-in/*p*-out polarisation. In situ SHG measurements were performed in a cell with a vertical Au working electrode of diameter 5 mm embedded in a Teflon cylindrical holder. The counter electrode was a Pt wire loop (1.25 cm^2) concentric and coplanar with the working electrode disc. An external Ag/AgCl reference electrode (RE) was used and placed in a separate compartment with the probe tip at 3 mm from the rim of the working electrode disc. The adequacy of this RE in the relevant experiments has been discussed insightfully in [12].

Results and discussion

In situ SHG measurements were carried out during two types of electrodeposition experiments: (a) a potential step was applied to the electrode, initially set at an anodic stripping potential, and (b) series of five potential square waves were applied between a fixed anodic stripping potential and a given cathodic polarisation.

As far as the choice of the optical polarisation is concerned, it is known [17, 18] that with *p*-polarisation, the output SHG bears strictly surface information, whilst with *s*-polarisation both surface and bulk information can be obtained. In our case, 'bulk' information can be estimated to derive from a layer of less than 100 nm. Thus, in the case of metal electrodeposition experiments—as opposed to adsorbate detection ones—such a thickness can be regarded to be typical of the 'surface' morphological growth features that we are interested in studying. Therefore—as hinted at in Section 2—our final polarisation choice was *p*-in/*p*-out for the highest sensitivity to the formation of Ag growth features. It is worth noting that it is possible that the diffuse signal from the electrode surface, roughened during electrodeposition, gives rise to insensitivity to both input and output polarisations [19].

In Figs. 1, 2 and 3, SHG signal intensity (I_{SHG}) transients—following the application of potentiostatic steps at cathodic over-potentials from an anodic stripping potential of 500 mV—are reported, using the electrodeposition baths (a), (b) and (c), described in Section 2. It can be noticed that, when the anodic potential is applied, I_{SHG} is high and essentially constant over time. The application of a cathodic step gives rise to an over-shoot, better visible in the systems containing CH_3CN and then to different I_{SHG} transient shapes, depending on the solvent and the imposed over-potential. The observed over-shoot is diagnostic of Ag nucleation processes on the gold substrate; for this reason, in all the investigated systems, the higher the over-potential, the lower the observed maximum of I_{SHG}, because of higher growth rate. In the aqueous solution, I_{SHG} decreases with time and tends to reach an asymptotic value, systematically decreasing with the increase of the cathodic polarisation (Fig. 1). In the two systems containing the organic solvent (Figs. 2 and 3), after the initial I_{SHG} over-shoot at lower cathodic over-potentials, an approximately constant value is reached, higher than the one observed at anodic potentials. At higher cathodic polarisations, I_{SHG} continues to decrease reaching, also in this case, an asymptotic value, anti-correlated with the applied cathodic over-potential. The critical over-potentials discriminating between the two different kinds of trend are −350 and −200 mV for the mixed electrolyte and for the pure organic solvent, respectively. The different types of I_{SHG} transient can be explained in terms of the formation of Ag nanoparticles, giving rise to a SHG signal enhancement, as detailed below. Unlike the measurements with pure solvents, experiments carried out in the mixed electrolyte give rise to serially correlated I_{SHG} transients, owing to the reaction of acetonitrile with water [11] causing an accumulation of reaction products.

In Figs. 4 and 5, we report I_{SHG} time series, obtained by applying a sequence of five potential square waves, consisting in switching the potential between an anodic stripping potential of 500 mV (over-potential η_1) and a given cathodic polarisation (η_2), with pure solvents. In Fig. 6, similar results are reported, obtained with the mixed electrolyte, for some representative cathodic potentials

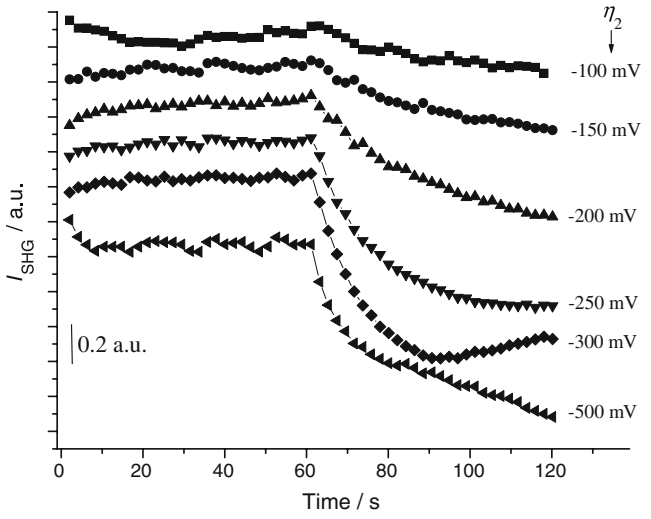

Fig. 1 SHG signal intensity transients following the application of potentiostatic steps at cathodic over-potentials (η_2) from an anodic stripping over-potential (η_1=+500 mV), using the electrodeposition bath containing $AgNO_3$ 10 mM, $NaClO_4$ 0.1 M and 100% H_2O

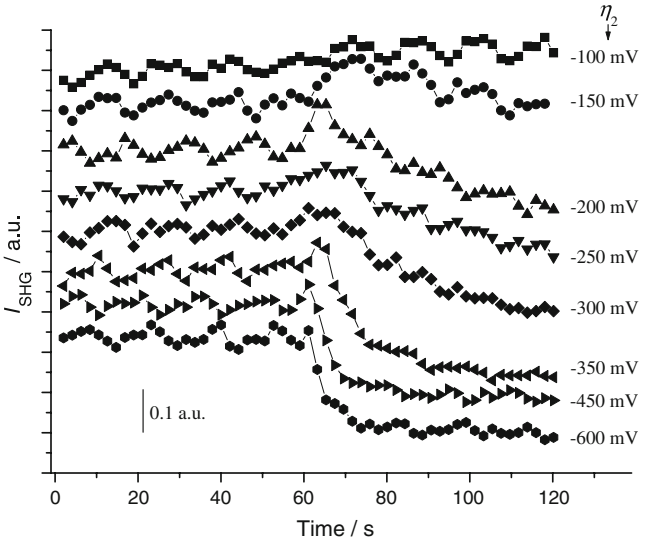

Fig. 3 SHG signal intensity transients following the application of potentiostatic steps at cathodic over-potentials (η_2) from an anodic stripping over-potential (η_1=+500 mV), using the electrodeposition bath containing $AgNO_3$ 10 mM, $NaClO_4$ 0.1 M and 100% CH_3CN

(−100, −300 and −600 mV). In the experiments with pure solvents, the I_{SHG} transients are more reproducible than with the mixed electrolyte, where the signal is affected by the CH_3CN reactivity. In particular, it is worth noting that, with the mixed solvent, the reproducibility is low at low η_2 values (Fig. 6a), it increases (even though in the presence of a drift) at higher η_2 (Fig. 6b) and it decreases again for very high η_2 values (Fig. 6c).

The change of I_{SHG} transient shapes for a given electrochemical condition, can be quantified by the parameter Δ, defined as $\Delta = \frac{1}{5N}\sum_{i=1}^{N}\sum_{j=1}^{5}\frac{A_{ij}-B_i}{A_{ij}}$, where A^{ij} are the I_{SHG} data collected during the j-th potential square wave, B_i are the I_{SHG} data collected during the single potential step and N is the number of time samples collected in each time series. Δ has been estimated to be 1.5–13%, depending on η_2, in the experiments with water, 1–15% with the organic solvent and more than 40% with the mixed electrolyte. Relatively higher Δ values are systematically found at higher over-voltages, likely owing to the build-up of deposit roughness.

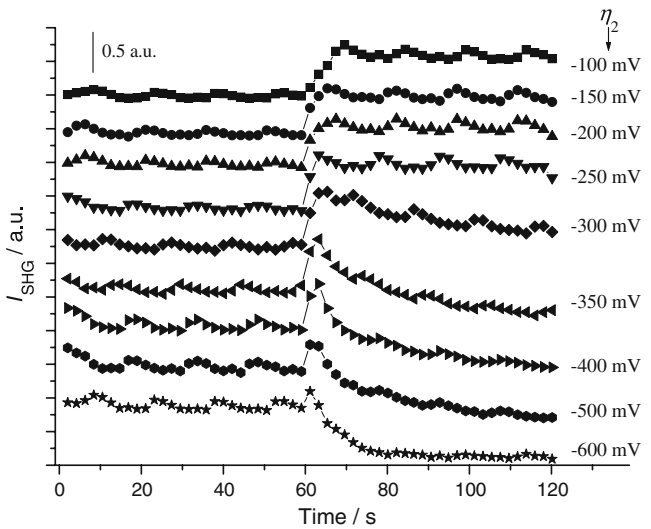

Fig. 2 SHG signal intensity transients following the application of potentiostatic steps at cathodic over-potentials (η_2) from an anodic stripping over-potential (η_1=+500 mV), using the electrodeposition bath containing $AgNO_3$ 10 mM, $NaClO_4$ 0.1 M, 50% H_2O and 50% CH_3CN

As hinted above, the anomalous behaviour of the I_{SHG} transients measured with the mixed electrolyte can be explained with the reactivity of acetonitrile during Ag electrodeposition, elucidated by SERS in [11]. In fact, as proposed in [20–22], under suitable conditions, CH_3CN can react with water, in two steps: (a) acetonitrile reacts with one water molecule to produce acetamide

$$CH_3CN + H_2O \rightarrow CH_3CONH_2 \quad (1)$$

and (b) acetamide reacts with another water molecule, yielding acetic acid and NH_3

$$CH_3CONH_2 + H_2O \rightarrow CH_3COOH + NH_3 \quad (2)$$

Ammonia tends to complex Ag^+ ions in the solution, producing the complexes $[Ag(NH_3)_2]^+$ and consequently reducing the Ag^+ activity and the electrodeposition rate.

In the presence of acetate, competition for Ag^+ takes place after the reaction:

$$Ag^+ + CH_3COOH \rightarrow CH_3COOAg \quad (3)$$

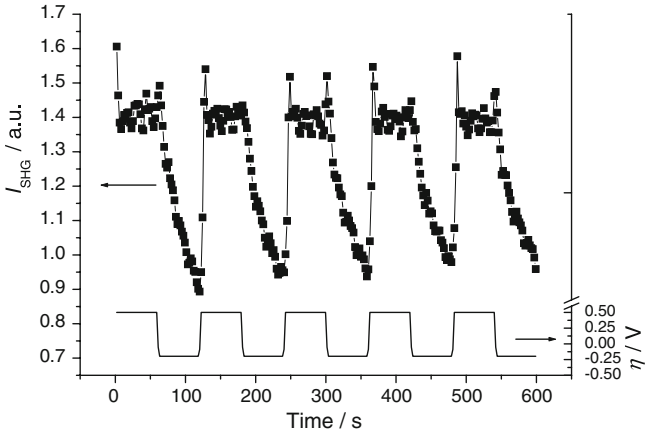

Fig. 4 I_{SHG} time series, obtained by applying a sequence of five potential square waves, switching the potential between an anodic stripping value of +500 mV and a cathodic polarisation of −200 mV, using the electrodeposition bath containing $AgNO_3$ 10 mM, $NaClO_4$ 0.1 M and 100% H_2O

CH_3COOAg is a sparingly soluble salt [23] and it tends to precipitate onto the electrode, giving rise to a passivation film, obstructing the stripping process of the silver electrodeposited during the anodic square waves (Fig. 6a).

When higher cathodic over-potentials η_2 are applied, CH_3CN tends to decompose releasing cyanide ions [11]:

$$CH_3CN \rightarrow CH_3^+ + CN^- \quad (4)$$

Cyanide ions CN^- can complex Ag^+ in the solution giving rise to $[Ag(CN)_2]^-$. The formation of the cyanocomplex, similarly to the case of the ammoniacal complex, reduces the activity of Ag^+ in the solution. Furthermore, cyanide ions injected in the solution by CH_3CN decomposition are good complexing agents for Ag^+, making the anodic stripping more efficient. In the presence of CN^- (Fig. 6b),

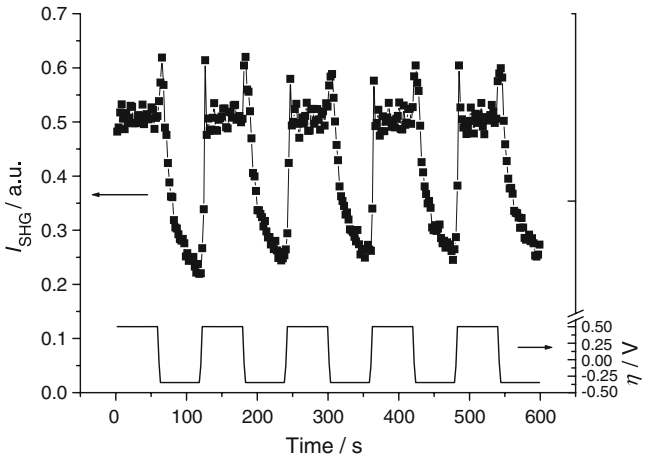

Fig. 5 I_{SHG} time series, obtained by applying a sequence of five potential square waves, switching the potential between an anodic stripping value of +500 mV and a cathodic polarisation of −350 mV, using the electrodeposition bath containing $AgNO_3$ 10 mM, $NaClO_4$ 0.1 M and 100% CH_3CN

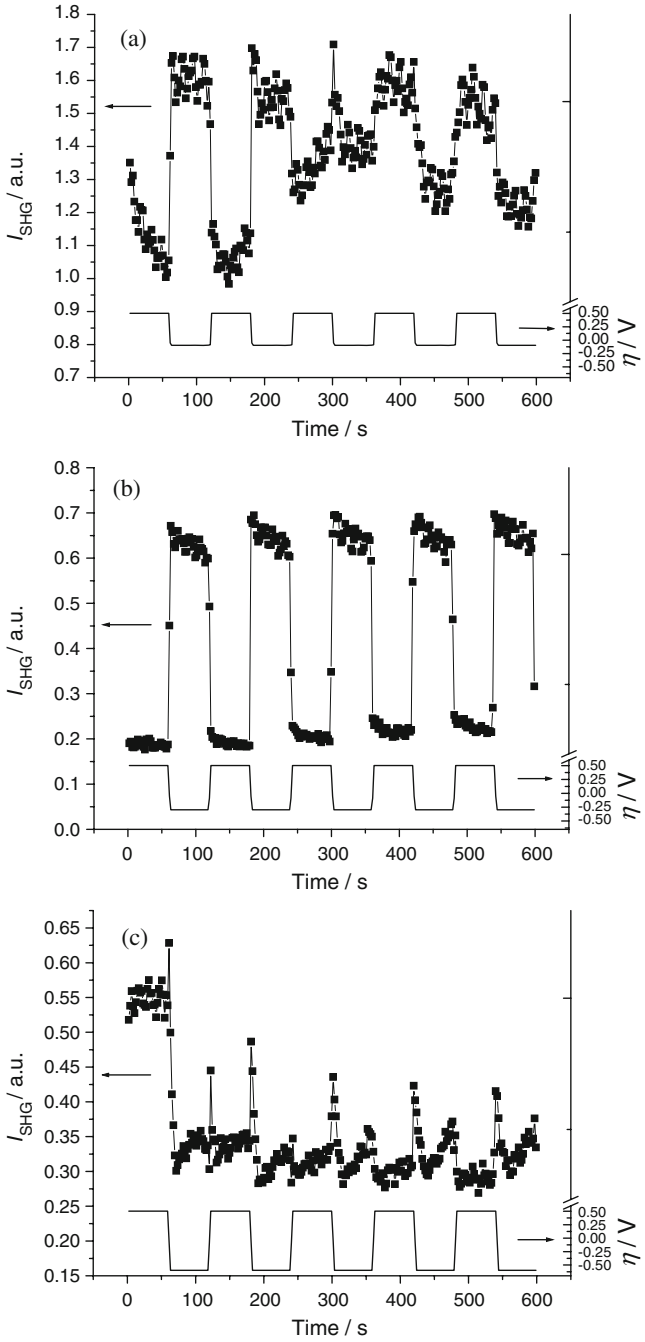

Fig. 6 I_{SHG} time series, obtained by applying a sequence of five potential square waves, switching the potential between an anodic stripping value of +500 mV and a given cathodic polarisation (over-potential η_2), using the electrodeposition bath containing $AgNO_3$ 10 mM, $NaClO_4$ 0.1 M, 50% H_2O and 50% CH_3CN. **a** η_2=−100 mV, **b** η_2=−300 mV, **c** η_2=−600 mV

in fact, the stripping time (60 s) is enough to restore the initial optical properties of the cathode. At even higher over-potentials η_2 (Fig. 6c), a hysteretic behaviour of the I_{SHG} transients can be observed, probably due to roughness effects.

In order to describe the non-linear optical response for a layer deposited onto a metal surface, a model based on the

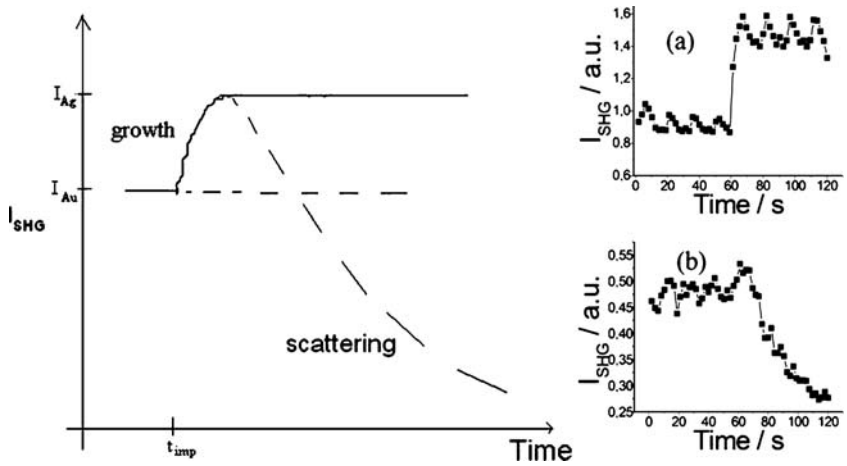

Fig. 7 A sketch of I_{SHG} dynamics, according to the model Eq. (7) and (8), with two typical I_{SHG} transients obtained in our measurements

theory reported in [1] has been adopted, introducing an additional damping term $\gamma(r)\dot{x}$. According to this model, based on the dynamic behaviour of the valence electrons of the over-layer [17, 24], the single electron equation is:

$$\ddot{x} + \gamma(r)\,\dot{x} - \omega_0^2 x + \zeta x^2 = \frac{e}{m}\{E(\omega)\cos(\omega t)\} \tag{5}$$

where ω_0 and ζ are the resonant frequency and anharmonicity of the potential field, respectively, and $E(\omega)$ is the magnitude of the oscillating electric field associated with the incident fundamental beam. In this case, the second-order non-linear susceptibility, $\chi^{(2)}$, is given by:

$$\chi^{(2)}(r) = -\zeta \frac{Ne^3}{2m^2} \frac{1}{\left[\left(\omega_0^2-\omega^2\right)^2+\gamma(r)^2\omega^2\right]\sqrt{\left(\omega_0^2-4\omega^2\right)+4\gamma(r)^2\omega^2}} \tag{6}$$

where $\chi^{(2)}(r)$ is a monotonically increasing function in the range $r \in [0;\infty)$.

If we assume that the absorption is due to plasmon resonance of metal nanoparticles, it is possible to monitor the nucleation and growth of crystallites. In fact, the variation of I_{SHG} can be expressed in terms of changes of the damping coefficient, written in turn as a function of particle size [25]. In order to calculate $\chi^{(2)}$, the dielectric function of silver can be determined by additive contributions of free and bound electrons [25, 26]. In our SHG experiments, at the excitation wavelength of 1,064 nm, the gold and silver responses are chiefly free electron-like [27] and can be described by the Drude model [25], obtaining:

$$\chi^{(2)}(r, \mathrm{Re}(\varepsilon^f)) = -\zeta \frac{Ne^3}{2m^2} \frac{1}{\left[(\omega_0^2-\omega^2)^2+\left[\frac{\omega_P^2}{1-\mathrm{Re}(\varepsilon^f)}-\omega^2\right]\omega^2\right]\sqrt{(\omega_0^2-4\omega^2)+4\left[\frac{\omega_P^2}{1-\mathrm{Re}(\varepsilon^f)}-\omega^2\right]\omega^2}} \tag{7}$$

Taking the relaxation time of the metal $\tau = 31\times10^{-15}$ s for Ag and $\tau = 9.3\times10^{-15}$ s for Au [28], one obtains $\frac{\chi^{(2)}_{Au}}{\chi^{(2)}_{Ag}} = 847$.

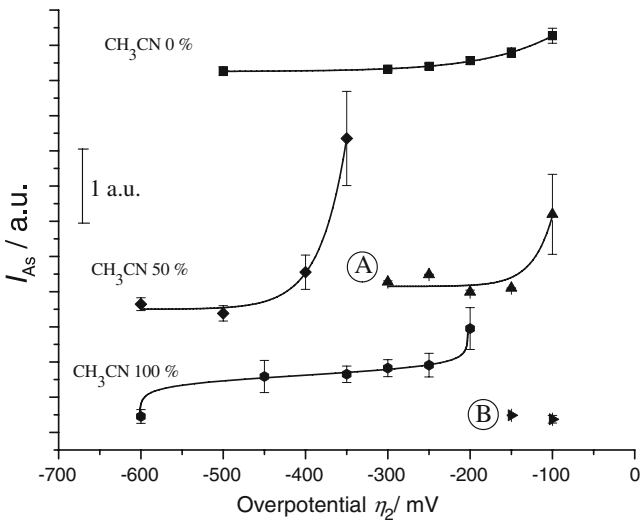

Fig. 8 Potential-dependent I_{as} and 95% confidence intervals estimated by non-linear least-squares (NLLS) fits of experimental I_{SHG} data (Eq. 8)

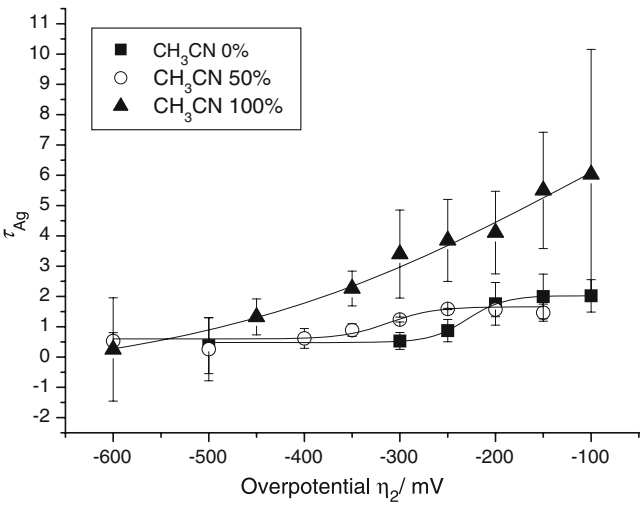

Fig. 9 Potential-dependent τ_{Ag} and 95% confidence intervals estimated by NLLS fits of experimental I_{SHG} data (Eq. 8)

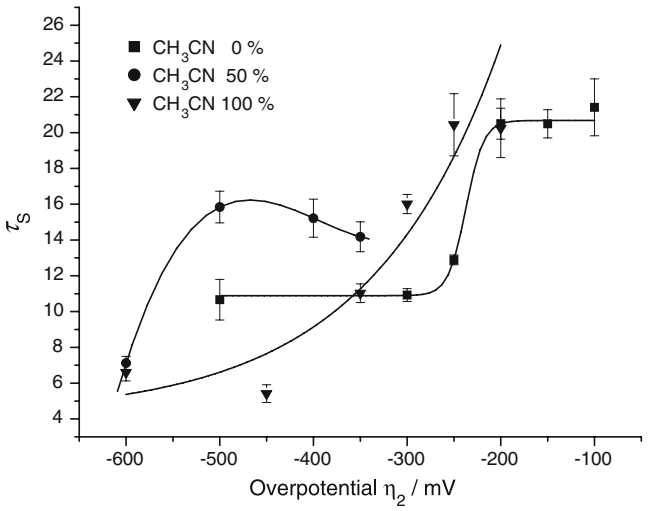

Fig. 10 Potential-dependent τ_s and 95% confidence intervals estimated by NLLS fits of experimental I_{SHG} data (Eq. 8)

According to this result, I_{SHG} from an atomically flat Au surface should be higher than that from an atomically flat Ag surface [27] and a fortiori from scattering Ag crystallites. Consequently, the over-shoots observed in our experiments can be explained in terms of enhanced SHG from Ag nanoparticles [29]. For spherical nanoparticles with radius r larger than 1 nm and smaller than the wavelength of light λ, *i.e. typically* $1\text{nm} < r < \frac{\lambda}{20}$ [30, 31], their SHG signal can be described by means of Eq. 7. This equation shows a positive correlation between $\chi^{(2)}$ and r in the range where the adopted approximations are valid. This single model permits to rationalise our experimental data. A conceptual sketch with two typical I_{SHG} transients obtained in our measurements is depicted in Fig. 7. During the initial period of 60 s, the recorded I_{SHG} corresponds to polished Au. When the cathodic potential step is applied (t_{imp}=60 s), the I_{SHG} signal increases due to the growth of Ag clusters onto the Au substrate. In the experiments where I_{SHG} increases above the Au level and stays approximately constant during the deposition process (Fig. 7, inset a), essentially monodisperse nanoparticles are formed [32–34]. The cases when the I_{SHG} signal decreases after the maximum (Fig. 7, inset b) can be explained with scattering from surface roughness, developing with the growth of Ag crystallites or dendrites.

The experimental I_{SHG} data, obtained in the different systems and by applying different cathodic polarisation sequences, have been normalised with respect to the average value of the signal corresponding to polished Au and have been fitted by means of the following function:

$$I_{SHG} = \left[1+I_{as}\left(1-\exp\left(-\frac{\bar{x}}{\tau_{Ag}}\right)\right)\right] \cdot \left[\exp\left(\frac{t_s-\bar{x}}{\tau_s}\right)\right] \qquad (8)$$

where I_{as} is the maximum value of the I_{SHG} signal or its asymptotic value, τ_{Ag} is the characteristic time of the initial growth of the signal, t_s is the time after which the effect of scattering is effective and τ_s is the characteristic I_{SHG} signal decay time for scattering. The estimates of I_{as}, τ_{Ag} and τ_s and their 95% confidence intervals are reported in Figs. 8, 9 and 10. In all the investigated systems, t_s has been found to be essentially equal to zero, indicating that the Ag clusters start contributing to the SHG scattering as soon as they form. The trend of the other parameters obtained by varying the cathodic over-potential can be explained in terms of formation of Ag nanoparticles, giving rise to SHG enhancement and their subsequent growth producing deposit roughness. The potential dependence of I_{as} is Butler–Volmer-like (Fig. 8), as expected for its dependence on the amount of the electrodeposited Ag. In fact, during the initial stages of electrocrystallisation, all the electrodeposited Ag can be assumed to give rise to the formation of SHG-active features, whilst at later stages, inactive and scattering crystallites tend to compete with optically active nanocrystals. Since the potential dependence of the duration of time interval preceding the descent of the I_{SHG} signal is rather weak, the amount of deposited Ag essentially scales with the current density, whence a hyperbolic-sine dependence of I_{as} on applied potential.

At lower over-potentials in the presence of an over-shoot, I_{as} allows to quantify the size of Ag nanoparticles. When the deposition rate is higher, the over-shoot is poorly visible and the I_{SHG} decay starts immediately. A clear discontinuity (points A and B in Fig. 8) can be noticed in the systems containing CH_3CN that can be related to the reactivity commented above (Eqs. 1 and 4) and corresponds to the resulting morphological effects.

The estimated data of τ_{Ag} show a monotonic trend (Fig. 9), with the cathodic over-potential step, and give information on the kinetics of metal growth.

An essentially positive correlation between the estimated τ_s values and the applied cathodic over-potential is found as expected for cathodic kinetics (Fig. 10). In particular, the system with mixed electrolyte seems slower, whereas the one with organic electrolyte is the faster.

Conclusions

Silver electrodeposition from water–acetonitrile mixed solvents has been investigated by means of SHG spectroscopy. This non-linear optical spectroscopy carried out during Ag electrodeposition provides a useful means for the study of the properties of Ag growth features. The different types of I_{SHG} transients, observed in our experiments, can be explained in terms of the formation of Ag nanoparticles, giving rise to SHG enhancement and their subsequent growth producing deposit roughness. Differences in the kinetics of Ag clusters formation and growth,

as a function of both chemistry and reactivity, as well as of the cathodic potential, can be detected and quantified with a simple optical model proposed in this work.

References

1. Corn RM, Higgins DA (1994) Chem Rev 94:107
2. Galus Z (1995) In: Gerischer H, Tobias CW (eds) Advances in electrochemical science and engineering. Wiley-VCH, Weinheim
3. Chen R, Xu D, Gao G, Gui L (2004) Electrochim Acta 49:2243
4. Gu R, Cao P, Sun YH, Tian Z (2002) J Electroanal Chem 528:121
5. Cao P, Gu R, Qiu L, Sun R, Ren B, Tian Z (2003) Surf Sci 531:217
6. Doubova LM, Daolio S, Pagura C, De Battisti A, Trasatti S (2003) Russ J Electrochem 39(2):164
7. Kuznetsov VV, Skibina LM, Loskutnikova IN (2000) Prot Met 36 (6):565
8. Kuznetsov VV, Skibina LM, Loskutnikova IN, Alekseev YE (2001) Prot Met 37(1):31
9. Peng X, Xiang C, Xie Q, Kang Q, Yao S (2006) J Electroanal Chem 591:74
10. Watanabe T (2004) Nano-plating. Elsevier, Tokyo
11. Mele C, Bozzini B (2008) J Solid State Electrochem. doi:10.1007/s10008-008-0724-y
12. Mele C, Bozzini B, Rondinini S, D'Urzo L, Romanello V, Tondo E, Minguzzi A, Vertova A (2008) J Solid State Electrochem. doi:10.1007/s10008-008-0732-y
13. Rusanova MY, Polášková P, Muzikař M, Fawcett VR (2006) Electrochim Acta 51:3097
14. Láng GG, Horányi G (2003) J Electroanal Chem 552:197
15. Láng G, Inzelt G, Vrabecz A, Horányi G (2005) J Electroanal Chem 582:249
16. Bozzini B, D'Urzo L, Mele C, Tondo E (2008) Galvanotecnica e nuove finiture 59:274
17. Shen YR (2003) The principles of nonlinear optics. Wiley, New York, p 497
18. Rubahn HG (2004) Nanophysik und nanotechnologie. Taubner, Stuttgart 77
19. Chen CK, De Castro ARB, Shen YR (1981) Phys Rev Lett 46:145
20. Venardou E, Garcia-Verdugo E, Barlow SJ, Gorbaty YE, Poliakoff M (2004) Vib Spectrosc 35:103
21. Lee GR, Crayston JA (1996) Polyhedron 15:1817
22. Luo RS, Mao XA, Pan ZQ, Luo QH (2000) Spectrochim Acta. Part A 56:1675
23. Cotton FA, Wilkinson G (1962) Advanced inorganic chemistry. Interscience, New York
24. Yariv A (1975) Quantum electronics. Wiley, New York
25. Oshchepkov SL, Sinyuk AF (1998) J Coll Interf Sci 208:137
26. Kolb DM (1988) In: Gale RJ (ed) Spectroelectrochemistry theory and practice. Plenum, New York, p 96
27. Guyot-Sionnest P, Tadjeddine A (1990) J Chem Phys 92:734
28. Johnson PB, Christy RW (1972) Phys Rev B 6:4370
29. Wokaun A, Bergman JG, Heritage JP, Glass AM, Liao PF, Olson DH (1981) Phys Rev B 24:849
30. Link S, El-Sayed MA (2000) Int Rew Phys Chem 19:409
31. Srinivasan R, Suni II (1999) J Electrochem Soc 146(2):570
32. Walters MJ, Pettit CM, Roy D (2001) Phys Chem Chem Phys 3:570
33. Pettit CM, Garland JE, Etukudo NR, Assiongbon KA, Emery SB, Roy D (2002) Appl Surf Sci 202:33
34. Nagy G, Roy D (1994) J Phys Chem 98:6592